

Zeolite-supported metal carbonyls: sensitive probes for infrared spectroscopic characterization of the zeolite surface

Carlos Otero Areán, Gemma Turnes Palomino, Estrella Escalona Platero and Margarita Peñarroya Mentrut

Departamento de Química, Universidad de las Islas Baleares, 07071 Palma de Mallorca, Spain

The metal carbonyls $[M(CO)_6]$ ($M = Mo$ or W) were found to be molecularly adsorbed on the surface of H-ZSM-5 zeolite crystals. Three types of adsorbed species were detected by IR spectroscopy: weakly physisorbed metal carbonyls and $[M(CO)_6]$ molecules interacting (*via* a CO ligand) with OH groups or with Lewis-acid sites (co-ordinatively unsaturated Al^{3+} ions). For physisorbed species a single C–O stretching mode (T_{1u}) was observed, around 1990 cm^{-1} . The $(OC)_3MCO \cdots HOSi$ species gave a band at 1965 cm^{-1} (anchored CO ligand) and the corresponding $E + 2A_1$ modes at higher frequency. O–Bonding between the metal hexacarbonyls and Lewis-acid centres gives rise to a characteristic IR absorption band in the range $1750\text{--}1850\text{ cm}^{-1}$, and corresponding $E + 2A_1$ modes at $\tilde{\nu}_{CO} > 2000\text{ cm}^{-1}$. Close inspection of these spectroscopic features, and comparison with IR spectra of adsorbed CO, enables characterization of the zeolite surface. For medium-pore zeolites an important feature of this method is that $[M(CO)_6]$ molecules cannot penetrate inside the zeolite channels, therefore discrimination between internal and external surface sites can be accomplished. Thus, it was found that both Brønsted-acid sites [bridged $Si(OH)Al$ groups] and silanols are located mainly inside the zeolite channels.

Zeolites and related microporous materials find wide application in a number of technological fields. Paramount among these is the use of zeolites as catalysts for the petrochemical industry, pollution control and the synthesis of speciality chemicals. They also serve as catalyst supports, ion exchangers and molecular sieves. The catalytically active sites of zeolites are mainly Brønsted acid OH groups, Lewis-acid sites associated with lattice defects or extra-framework material and heteroatoms (such as Fe, Ga or Ti) which can substitute for Al in the aluminosilicate framework. These sites can be located either inside channels or at the external surface of the solid particles. In more general terms, most applications of zeolites rest on processes occurring at their surfaces, either internal (intra-crystalline pores and cavities) or external. Therefore, detailed characterization of these surfaces is required for a deep understanding of zeolite properties and behaviour. To this end, a prime requirement is to differentiate between internal and external surfaces, and appropriate means must be devised to accomplish this task.

We show here how the combined use of two IR spectroscopic probes, CO and an appropriate metal carbonyl, $[Mo(CO)_6]$ or $[W(CO)_6]$, can help to render zeolite surfaces IR-readable and to differentiate external from internal features. Recent accounts on the use of small molecules (*e.g.* H_2 , N_2 , CO, pyridine) as IR spectroscopic probes can be found in the literature.¹ A different approach was taken by several authors^{2–7} who used magic angle spinning (MAS) NMR and photoelectron spectroscopy. Our results are in broad agreement with theirs.

As a case study the protonic form of ZSM-5 will be considered. This is an MFI-type⁸ silicon-rich zeolite which has a three-dimensional channel system with openings of about 0.55 nm in diameter, defined by ten-membered rings of TO_4 tetrahedra^{9,10} ($T = Si$ or Al). Carbon monoxide, which has a kinetic diameter of 0.376 nm, finds free access to the intracrystalline space, and this molecule is very often used as an IR spectroscopic probe for zeolite characterization.¹¹ However, simultaneous interaction with the external surface of the zeolite crystals renders discrimination between internal and external sites very difficult. The octahedral $[Mo(CO)_6]$ and $[W(CO)_6]$ molecules have molecular dimensions of about 0.75 nm,¹² and thus they can only probe external surfaces.

Although zeolite characterization is the main purpose of the

present work, a second aim was to carry out a detailed study of the interaction of the metal carbonyls with the (external) zeolite surface. This is relevant to the developing field of surface organometallic chemistry, which deals with the structure and reactivity of supported metal complexes and organometallic compounds. The key factor in this field is that the presence of a surface reduces the dimensionality of the ensuing reactions, and it can also result in directing stereochemistry, stabilizing reaction intermediates or facilitating activation of adsorbed molecules.¹³ Characterization of the adsorbed species should be the first step in this line of research.

Experimental

The sodium form of ZSM-5 was prepared by template-assisted hydrothermal synthesis, using appropriate amounts of sodium silicate, aluminium nitrate and tetrapropylammonium bromide solutions (Aldrich Chemicals, 99.99% purity). Preparation of the parent gel mixture, having a Si:Al ratio of 15:1, was accomplished following standard procedures.¹⁴ This gel was then placed inside an autoclave with a Teflon lining and heated under autogenous pressure for 6 d at 443 K; the resulting product was thoroughly washed with distilled water and allowed to dry in air at room temperature. Thermal decomposition of the organic template was achieved by calcination at 773 K for 5 h, using at the end of the calcination period an oxygen flow to burn off residual coke. Ionic exchange with a 0.5 mol dm^{-3} ammonium nitrate solution led to the ammonium form of the zeolite, which was then thermolysed (at 673 K) to yield the corresponding protonic H-ZSM-5 form. Sample crystallinity and phase purity was examined by powder X-ray diffraction, while transmission electron microscopy (TEM) was used to examine the sample morphology and particle size.

For IR studies, thin self-supporting wafers of the parent sample were prepared and activated in a vacuum for 2 h inside IR cells which allowed *in situ* high-temperature treatment, gas dosage, and room- or low-temperature IR measurements to be made. For low-temperature (77 K) measurements of carbon monoxide adsorption we used a quartz cell (similar to that described by Marchese *et al.*¹⁵) fitted with NaCl windows, which was permanently cooled with liquid nitrogen. A similar cell

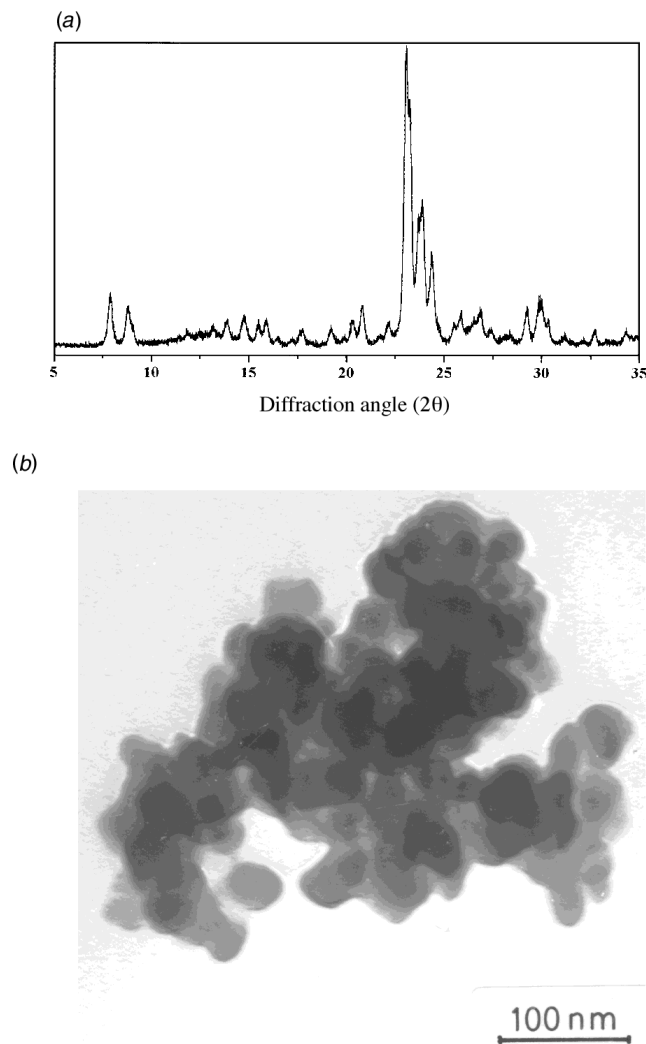


Fig. 1 (a) Powder X-ray diffraction pattern (Cu-K α radiation) of the H-ZSM-5 sample. (b) Representative TEM micrograph showing the morphology of the zeolite powder

(without cooling) was used to obtain room-temperature spectra of the adsorbed metal carbonyls. Increasing amounts of these carbonyls were dosed by sublimation at room temperature from a side arm of the IR cell. Transmission IR spectra were recorded, at 3 cm^{-1} resolution, on a Bruker IFS 66 FTIR spectrometer.

Results and Discussion

Structural and morphological characterization of the zeolite sample

The synthesized zeolite sample was found to give an X-ray diffraction pattern, shown in Fig. 1(a), where all diffraction lines could be assigned to a single phase having the ZSM-5 (MFI) structure type.¹⁴ The observed broadness of the diffraction lines is presumably due to the very small crystal size, as seen by electron microscopy. No other crystalline by-products could be detected within the experimental accuracy of the diffraction method used. This, however, does not exclude the possible presence of a small proportion of amorphous material, which would escape detection by X-ray diffraction. The diffractograms of zeolite wafers were not found to change upon thermal treatments.

Fig. 1(b) shows a representative micrograph of the zeolite crystals. The solid consists of loose aggregates of spheroidal particles, which have a rather uniform size of about 30 nm in

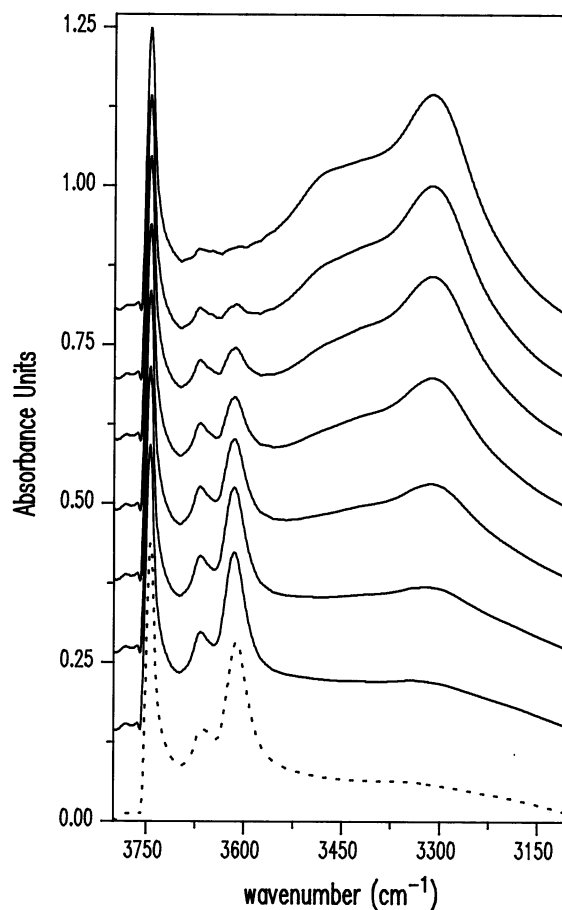
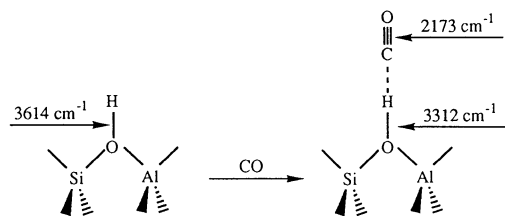
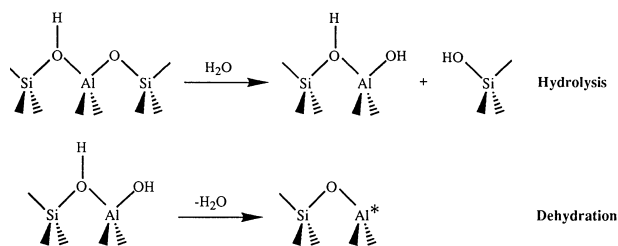


Fig. 2 Infrared spectra in the O-H stretching region of H-ZSM-5 outgassed at 723 K (broken line) and the effect of increasing doses (from 10^{-2} to 20 Torr) of CO at 77 K

diameter. This small particle size suggests that external surfaces should contribute significantly to surface-related properties of the zeolite sample.

Characterization by Fourier-transform IR spectroscopy: O-H stretching region

For IR characterization a thin wafer of the H-ZSM-5 sample was activated (inside the IR cell) at 723 K for 2 h under a dynamic vacuum: residual pressure $< 10^{-4}$ Torr (1 Torr = 133.3 Pa). Infrared spectra taken at 77 K are shown in Fig. 2, which depicts the original zeolite spectrum and the effect of increasing doses of CO. The zeolite blank spectrum shows two main IR absorption peaks: 3745 and 3614 cm^{-1} , and a weak band at 3669 cm^{-1} . There is general agreement in the literature¹⁶ that the peak at 3745 cm^{-1} corresponds to silanols while that at 3614 cm^{-1} is the O-H stretching of bridged Si(OH)Al groups (Brønsted-acid sites). The weak band at 3669 cm^{-1} is assigned, in agreement with previous reports,^{4,16b,e,17} to hydroxyl groups attached to extra-framework aluminium. These extra-framework species could be formed in several processes. In the first place incomplete crystallization of the parent gel during zeolite synthesis could leave non-negligible amounts of amorphous aluminium hydroxides, or hydroxide oxides which would escape detection by X-ray diffraction. Template burning is also a process which can lead to formation of local defects exposing coordinatively unsaturated Al^{3+} ions (see later) and Al-OH groups. Finally, thermal activation of the zeolite very often leads to partial hydrolysis of Si-O-Al bonds, as depicted in Scheme 1. Note that dehydration is expected to proceed at a higher temperature than the hydrolysis step. The Al* atom in Scheme 1 is at a lattice defect where the zeolite framework has been disrupted, but not yet in a complete extra-framework pos-



ition. However, hydrolysis does not necessarily stop at the stage shown in Scheme 1; it can continue up to the point where all bonds linking the Al atom to the framework are broken, with attendant formation of extra-framework Al(OH)₃ or AlO(OH) species which can then aggregate, and be dehydroxylated, to a varying extent. All of these processes explain why a weak IR absorption band at about 3655–3670 cm⁻¹ is clearly observed^{16e} in some preparations, while in others it is much weaker or does not exist at all.

Adsorption of CO, at 77 K, results in progressive erosion of the band at 3614 cm⁻¹ and parallel growth of a wider and more intense IR absorption band with a maximum at 3312 cm⁻¹. This is due to formation of a hydrogen-bonded adduct, as depicted in Scheme 2. This phenomenon has been extensively discussed in the literature,^{11,16b,e,18,19} so that only this brief description is given here with the double purpose of (i) completing the characterization of the zeolite sample used, and (ii) facilitate understanding of the metal carbonyl spectra discussed later. Note, however, that discrimination between Brønsted-acid sites located inside channels or at external surfaces is not possible at this stage, since CO has direct access to both of them.

The band at 3669 cm⁻¹ is also eroded upon interaction with CO and, at the highest doses, the silanol band (3745 cm⁻¹) is also slightly affected. Both of these phenomena have been previously discussed.^{11,16e}

C–O Stretching region of adsorbed carbon monoxide

Fig. 3 shows the C–O stretching region of carbon monoxide adsorbed on H-ZSM-5 previously activated at 723 K. At small doses of CO, a main IR absorption band is observed at 2173 cm⁻¹ which corresponds¹¹ to the C–O stretching of hydrogen-bonded CO (Scheme 2). A weaker, and complex, band appears in the 2210–2240 cm⁻¹ range with a maximum at 2228 and a clear shoulder at 2221 cm⁻¹ (see inset in Fig. 3). This band, which saturates at low doses, is assigned to the C–O stretching of Al³⁺···CO adducts formed on dehydroxylated (Al₂O₃) extra-framework species. A similar feature was observed for many zeolites activated at high temperature, and similarly assigned.^{11,16g,20} It was also found for CO adsorbed on γ -alumina.^{15,21,22} Note that the composite nature of the band strongly suggests the presence of two types (or families) of coordinatively unsaturated Al³⁺ ions. They should correspond to edges and corners of very small crystallites (high-frequency component) and to Al³⁺ ions situated in extended faces (low-frequency component). Partially extra-framework Al³⁺ ions (trigonal Al* species in Scheme 1) could also contribute to the

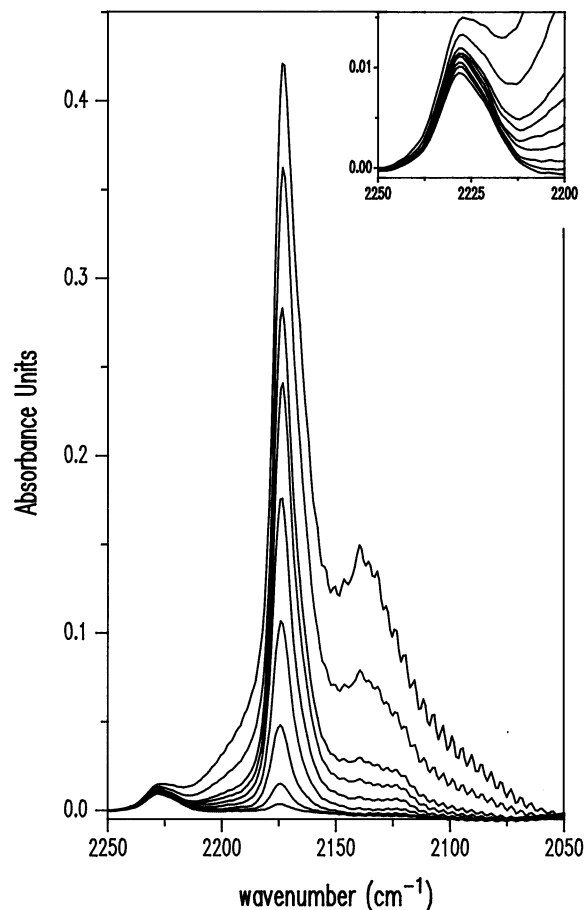


Fig. 3 Infrared spectra of adsorbed CO in the C–O stretching region (cf. Fig. 2); the zeolite blank was subtracted. Inset shows an enlarged view of the 2200–2250 cm⁻¹ region

2228 cm⁻¹ component. Finally, Fig. 3 also shows that for high doses of CO a broad band develops around 2138 cm⁻¹. This band, which shows a roto-vibrational profile, corresponds to weakly physisorbed (liquid-like) CO inside the zeolite channels.^{16g,21,23}

IR Spectra of adsorbed metal carbonyls: external surface sites

Fig. 4 shows the IR spectra, in the C–O stretching region, of [W(CO)₆] adsorbed at increasing doses on H-ZSM-5 previously activated at 723 K for 2 h in vacuum. Corresponding spectra in the O–H stretching region are depicted in Fig. 5. The nature of the adsorbed surface species can be discerned by first considering some brief theoretical arguments.

Free [W(CO)₆], point group *O_h*, has a single IR-active C–O stretching mode of *T_{1u}* symmetry at \approx 2000 cm⁻¹. The corresponding *E_g* and *A_{1g}* modes, being only Raman active are not observed in the IR spectra. The same applies to a weakly physisorbed [M(CO)₆] carbonyl, although the *E_g* and *A_{1g}* modes could become slightly active when the perturbation caused by the adsorbent is significant. Specific interaction of [M(CO)₆] with surface sites of metal oxides and zeolites is known²⁴ to lead to formation of Lewis-type adducts, where a CO ligand of the metal carbonyl interacts (*via* the oxygen atom) with surface OH groups or with co-ordinatively unsaturated metal ions (surface Lewis-acid sites). The surface-anchored metal carbonyl has *C_{4v}* symmetry, and a vibrational representation $\Gamma_{\text{CO, str}} = 2A_1 + E + B_1$, where the $2A_1 + E$ modes are IR active. In addition, a low-frequency band is also expected which would correspond to the anchoring CO ligand.^{24–26} The bathochromic shift of this C–O stretching mode is correlated with the hypsochromic shift of the remaining carbonyl ligands.^{24,26} This is summarized in

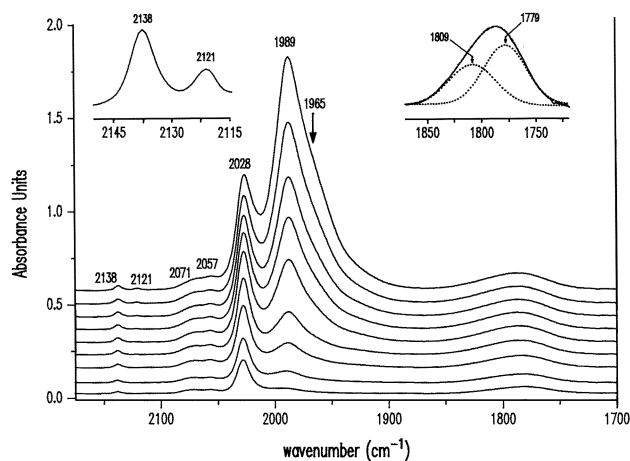


Fig. 4 Infrared spectra of successive doses (ca. 0.1 Torr) of $[\text{W}(\text{CO})_6]$ on H-ZSM-5. Sample previously outgassed at 723 K. The right-hand side inset shows computer deconvolution of the low-frequency band. The left-hand inset is an enlarged view of the 2115–2145 cm^{-1} region corresponding to the last dose of the metal carbonyl

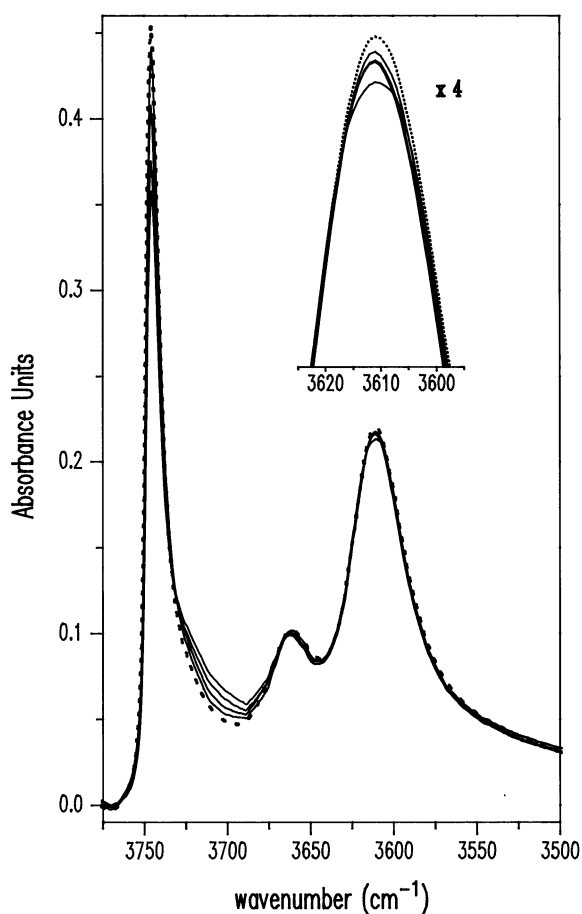


Fig. 5 Effect of increasing doses of $[\text{W}(\text{CO})_6]$ on the O–H stretching region. The broken line represents the zeolite blank spectrum. Inset shows an enlarged detail of the band at 3614 cm^{-1}

Scheme 3, which can help in the discussion of the IR spectra of the adsorbed species.

The band at 1989 cm^{-1} in Fig. 4, which becomes dominant at high doses of $[\text{W}(\text{CO})_6]$, is assigned to the T_{1u} mode of weakly (non-specifically) physisorbed metal carbonyl. This assignment is consistent with the fact that upon outgassing the IR cell for a few minutes at room temperature the intensity of the band at 1989 cm^{-1} decreases very rapidly, as shown in Fig. 6. The shoulder at 1965 cm^{-1} is assigned to the C–O stretching of the

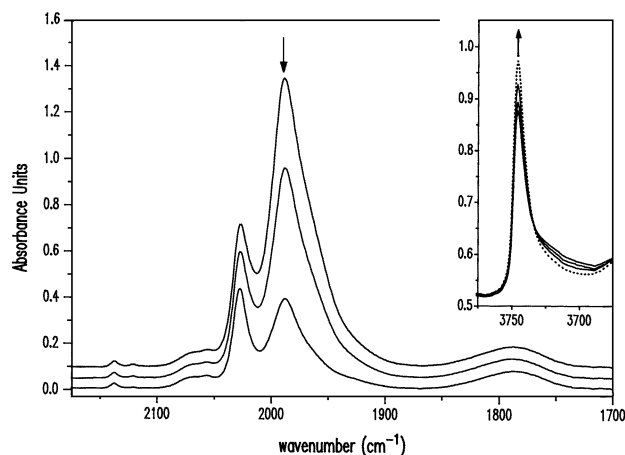
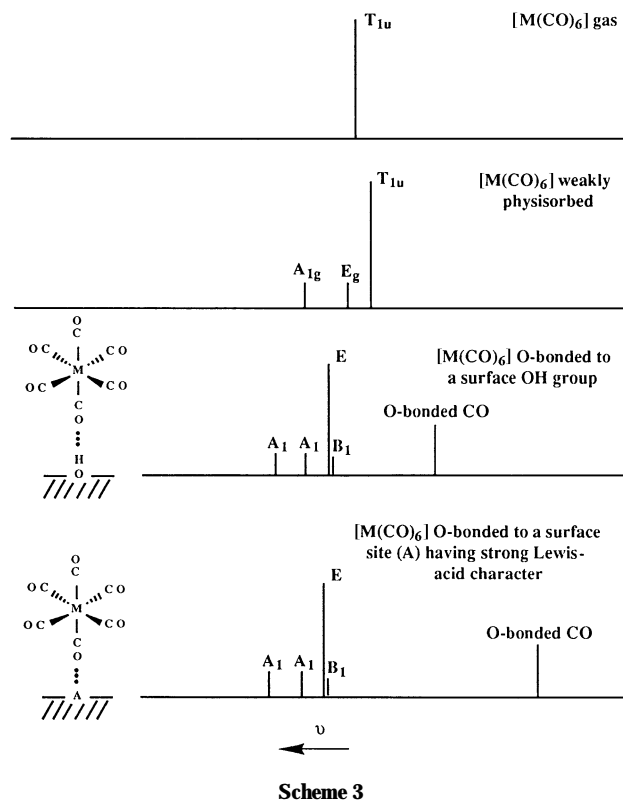
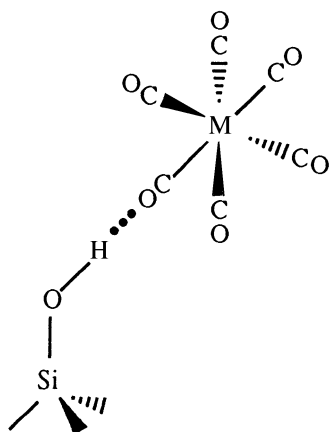


Fig. 6 Effect of outgassing the IR cell for 1 and 3 min after adsorption of a large dose of $[\text{W}(\text{CO})_6]$. The inset shows the corresponding spectra for the silanol band at 3745 cm^{-1} ; the broken line represents the zeolite blank

carbonyl ligand interacting with a surface silanol in the species depicted in Scheme 4. The corresponding E mode is very likely overshadowed by the band at 1989 cm^{-1} , while the two A_1 modes are the weak band at 2121 cm^{-1} and a second one at about 2030 cm^{-1} (see later) which is masked by the stronger band at 2028 cm^{-1} . The IR spectra in the O–H stretching region (Fig. 5) provide clear evidence for this assignment. Upon adsorption of the metal carbonyl the silanol band at 3745 cm^{-1} is partially eroded and shifted (with considerable broadening) to the 3680–3725 cm^{-1} region. This is the classical effect of a hydrogen-bonded interaction,²⁷ as depicted in Scheme 4. Note also that upon outgassing the metal carbonyl the initial intensity of the band at 3745 cm^{-1} is steadily recovered, as shown in the inset of Fig. 6.

The broad band observed in the 1750–1850 cm^{-1} region (Fig. 4) is assigned to the C–O stretching of the O-bonded carbonyl ligand of more strongly chemisorbed $[\text{W}(\text{CO})_6]$ spe-



Scheme 4

cies, as depicted in Scheme 3 (bottom diagram). Infrared absorption bands in this region were also reported, and similarly assigned, for Group 6 metal carbonyls adsorbed on γ -alumina.²⁸ Note that this band (which is strongly asymmetrical) mirrors that at 2210–2240 cm^{-1} in Fig. 3, which was assigned to CO adducts formed on aluminium extra-framework species. As in that case, the band at 1750–1850 cm^{-1} can also be resolved into two components with maxima at 1779 and 1809 cm^{-1} , as shown in the right-hand inset of Fig. 4. This implies that two families of chemisorbed metal carbonyl species should be present. The corresponding E modes are not individually resolved: they add up to give the (complex) band at 2028 cm^{-1} . The A_1 modes are clearly resolved at 2057 (which corresponds to the species giving the 1809 cm^{-1} component) and at 2071 cm^{-1} (low-frequency partner at 1779 cm^{-1}). The two remaining A_1 modes are observed (unresolved) at 2138 cm^{-1} . Note that on partial desorption of the metal carbonyl (Fig. 6) all of these bands are more resistant than those corresponding to the more weakly held surface species, as expected. They also grow first with the initial doses of the metal carbonyl (Fig. 4).

Regarding characterization of the zeolite, the following main points emerge from careful inspection of Fig. 5. (i) The IR absorption band at 3669 cm^{-1} is not affected by adsorption of the metal carbonyl. (ii) The band at 3614 cm^{-1} , corresponding to Brønsted acid Si(OH)Al groups is only very slightly eroded. (iii) The silanol band at 3745 cm^{-1} is significantly eroded, but much of it remains after adsorption of $[\text{W}(\text{CO})_6]$. Note that no further changes in the O–H stretching region of the spectra were observed after dosing the zeolite wafer with a very large excess of the metal carbonyl (spectrum not shown).

Since the diameter of the $[\text{W}(\text{CO})_6]$ molecule is greater than the free entrance dimension of the zeolite channels, the foregoing experimental facts demonstrate the following points. (i) The species giving rise to the O–H stretching at 3669 cm^{-1} are occluded inside the zeolite channels. (ii) Bridging OH groups (Brønsted-acid sites) are mainly internal (note that they were probed by CO), but a small fraction is located at the external surface of the zeolite crystals. This is relevant to catalysed processes where external acid sites could have an important role; for instance in the isomerization of substituted xylenes and styrenes.²⁹ Note that, although a very small effect is observed in the O–H stretching band at 3614 cm^{-1} , the concentration of the corresponding adsorbed species seems to be too small to give distinctive features in the carbonyl region of the IR spectra (Fig. 6). (iii) Silanols are located both at external surfaces {affected by $[\text{W}(\text{CO})_6]$ adsorption} and inside the zeolite channels (not accessible to the metal carbonyl). This point will now be considered further.

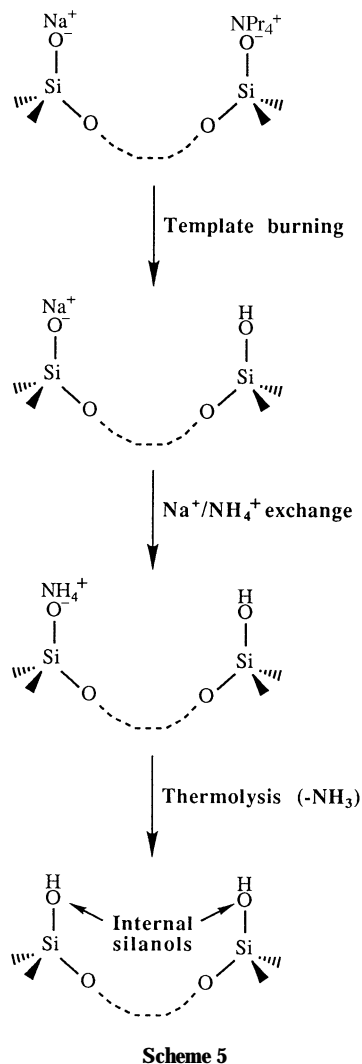
In an idealized zeolite crystal silanols would only occur at the

external surface, where they saturate dangling bonds created by truncation of the framework. The presence of silanols inside the channels can be accounted for by (i) lattice defects arising from partial dealumination, and (ii) the presence of a small fraction of amorphous silica which would escape detection by X-ray diffraction. This amorphous material could be occluded in the intracrystalline space of the zeolite, and the corresponding silanols would also give an IR absorption band^{30–32} at around 3745 cm^{-1} . However, the fraction of internal silanols revealed by our experiments seems to be too large to be explained on these terms. Although precise quantitative measurements are precluded, because of uncertainty about where to draw the baseline of the band at 3745 cm^{-1} (Fig. 5), our approximate values indicate that at least 70% of the integrated intensity of this band remains unaltered after adsorption of $[\text{W}(\text{CO})_6]$. This finding is in broad agreement with reported results from MAS NMR studies. Several authors^{4,5,33} have found that the ^{29}Si NMR signal corresponding to silanols in H-ZSM-5 samples is much greater (by at least one order of magnitude) than the value obtained from a calculation of the concentration of SiOH groups at the crystal faces. Although these calculations involve some degree of approximation regarding the morphology of the zeolite crystals and the value obtained depends also on the crystal size (about 1 μm in the reported NMR studies), the fact remains that internal silanols are much more abundant than is often assumed. A large concentration of internal silanols can be explained by carefully considering the processes taking place during zeolite synthesis.

It has been proposed by Boxhoorn *et al.*³³ that the zeolite framework acts as a charge-balancing counter ion for Na^+ and NPr_4^+ cations present in the parent gel (NPr_4^+ ions come from the tetrapropylammonium bromide used as a templating agent). The presence of NPr_4^+ ions associated with SiO^- defect centres would result in frustrated ring closure, as envisaged in Scheme 5 which also shows how after template burning, ion exchange and thermolysis (to yield the protonic form of the zeolite) internal silanols are created. Further evidence in favour of this process (which explains a high concentration of internal silanols) comes from cross polarization (CP) MAS ^{13}C NMR studies by Boxhoorn *et al.*³⁴ showing that NPr_4^+ ions remain intact during zeolite synthesis, while chemical analysis shows that the as-synthesized zeolite did not contain occluded Br^- ions. Also, ^{29}Si MAS NMR spectra reported by Engelhardt *et al.*³⁵ give evidence for the presence of SiO^- centres in the zeolite framework: $\delta -103$.

While internal silanols are not probed by $[\text{W}(\text{CO})_6]$, adsorbed CO should have free access to isolated SiOH groups both internal and external. However, in agreement with previous reports¹⁶ carbon monoxide was found to produce only a very small effect (faint erosion) of the band at 3745 cm^{-1} (Fig. 2). This can be explained in terms of the lability of the $\text{SiOH}\cdots\text{CO}$ adducts, because of the low basicity and high mobility of the CO molecule. In other words, formation of $\text{SiOH}\cdots\text{CO}$ adducts can be considered as a dynamic equilibrium where non-perturbed (or very weakly perturbed) silanols are always dominant. However, it seems unlikely that a similar consideration would apply to adsorbed $[\text{W}(\text{CO})_6]$, which should cause perturbation of all external silanols, particularly at high overdoses.

Let us now consider characterization of extra-framework species. Since these species are known to form mainly during thermal activation of the zeolite, it was considered interesting to compare results obtained for the sample activated at 723 K with corresponding data for a sample treated at a lower temperature. Fig. 7 shows the IR spectra of $[\text{Mo}(\text{CO})_6]$ adsorbed at increasing doses on H-ZSM-5 activated at 473 K for 2 h in a dynamic vacuum (inside the IR cell). Molybdenum hexacarbonyl was chosen this time to test the general validity of the results obtained with $[\text{W}(\text{CO})_6]$.



Comparison between Figs. 7 and 4 shows that for the zeolite sample activated at 473 K the complex band in the 1750–1850 cm^{-1} region is no longer present. Consequently, the related peaks at 2028, 2057, 2071 and 2138 cm^{-1} (Fig. 4) have disappeared from the spectra in Fig. 7. This confirms the previous assignment of these bands to strongly chemisorbed $[\text{W}(\text{CO})_6]$ in the sample activated at 723 K. The IR spectra of $[\text{Mo}(\text{CO})_6]$ adsorbed on the sample treated at 473 K (Fig. 7) show only a strong band at 1995 cm^{-1} , assigned to weakly physisorbed species, the shoulder at 1965 cm^{-1} (which is now more distinctive than in Fig. 4) and two remaining bands at 2030 and at 2121 cm^{-1} . These two bands, together with the shoulder at 1965 cm^{-1} , were previously assigned to C–O stretching modes of the metal carbonyl interacting with surface silanols (see Schemes 3 and 4). It was also seen (spectra not shown) that the silanol band at 3745 cm^{-1} was partially eroded upon adsorption of the metal carbonyl, much the same as shown in Fig. 5 for adsorbed $[\text{W}(\text{CO})_6]$. It is thus confirmed that both metal hexacarbonyls are molecularly adsorbed on the zeolite, and that they form corresponding adducts with surface silanols.

The absence of the band at 1750–1850 cm^{-1} (and corresponding high-frequency peaks) from the IR spectra in Fig. 7 demonstrates that extra-framework (aluminium oxide) species which molecularly chemisorb $[\text{W}(\text{CO})_6]$ (revealed in the spectra of Fig. 4) were formed during activation of the zeolite at 723 K. Thermal treatment at 473 K does not generate these species. Note also that IR spectra (not shown) of CO adsorbed at 77 K on the zeolite sample treated at 473 K did not display the band at 2210–2240 cm^{-1} (cf. Fig. 3).

Regarding the location of the extra-framework species, we note that they were probed by both adsorbed molecules, CO

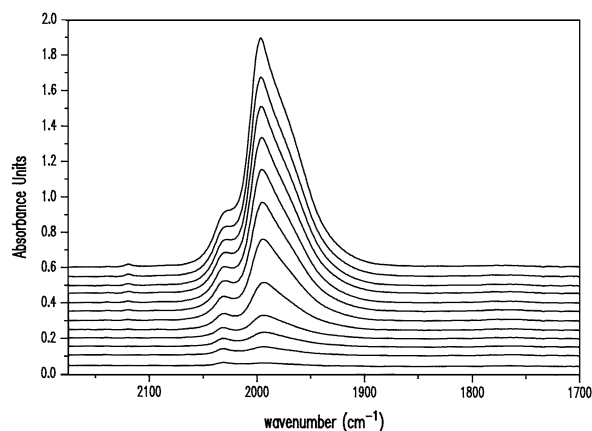


Fig. 7 Infrared spectra of $[\text{Mo}(\text{CO})_6]$ on H-ZSM-5 at increasing dosage of the metal carbonyl. Zeolite sample previously outgassed at 473 K

and $[\text{W}(\text{CO})_6]$, although the metal hexacarbonyl is a more sensitive probe: compare the intensity of the bands at 2210–2240 (Fig. 3) and at 1750–1850 cm^{-1} (Fig. 6). At least a significant fraction of these species should be located at external surfaces, since they are probed by $[\text{W}(\text{CO})_6]$, but there could also be an internal fraction. Carbon monoxide does not discriminate between internal and external sites, but comparison between the spectroscopic manifestations of CO and $[\text{W}(\text{CO})_6]$ could lead to quantification of both groups. However, in order to do this, absorption coefficients for the relevant IR bands {2210–2240 cm^{-1} for adsorbed CO and 1750–1850 cm^{-1} for $[\text{W}(\text{CO})_6]$ } had to be known. At present this is not the case.

Conclusion

The complexes $[\text{Mo}(\text{CO})_6]$ and $[\text{W}(\text{CO})_6]$ are molecularly adsorbed (at room temperature) on H-ZSM-5; no evidence for partial decarbonylation was observed in the corresponding IR spectra. The metal hexacarbonyls interact, *via* a CO ligand, with surface OH groups and co-ordinatively unsaturated Al^{3+} ions located at the external surface of the zeolite crystals. These interactions lead to perturbation of the C–O and O–H stretching modes which makes the external surface of the zeolite crystals IR-readable. Discrimination between internal and external sites rests on the fact that the metal carbonyls have a molecular size greater than that of the free entrance to the zeolite channels. By the combined use of CO and the metal hexacarbonyls as IR spectroscopic probes the following main points were shown. (i) A large proportion of silanols (at least 70%) are internal, which is in agreement with data reported from NMR studies but contrary to the idealized model of the zeolite structure. (ii) Brønsted-acid sites [bridged $\text{Si}(\text{OH})\text{Al}$ groups] are mainly internal, but a non-negligible fraction is located at external surfaces. (iii) During thermal activation of the zeolite at 723 K extra-framework (aluminium oxide) species are formed which have a substantial presence at external surfaces, although they can also be present inside the zeolite channels.

Acknowledgements

This work has been supported by the Spanish Dirección General de Investigación Científica y Técnica (PB93–0425). The Spanish Ministerio de Educación y Ciencia is gratefully acknowledged for a fellowship (to G. T. P.).

References

- See, for example: J. A. Lercher, C. Gründling and G. Eder-Mirth, *Catal. Today*, 1996, **27**, 353; H. Knözinger, in *Elementary Reaction Steps in Heterogeneous Catalysis*, eds. R. W. Joyner and R. A. van

- Santen, Kluwer, Amsterdam, 1993, p. 267; V. Gruver and J. J. Fripiat, *J. Phys. Chem.*, 1994, **98**, 8549; K. M. Neyman, P. Strodel, S. Ph. Ruzankin, N. Schlensog, H. Knözinger and N. Rösch, *Catal. Lett.*, 1995, **31**, 273; M. Jiang and H. G. Karge, *J. Chem. Soc., Faraday Trans.*, 1996, 2641; T. Barzetti, E. Selli, D. Moscotti and L. Forni, *J. Chem. Soc., Faraday Trans.*, 1996, 1401; G. Turnes Palomino, C. Otero Areán, F. Geobaldo, G. Ricchiardi, S. Bordiga and A. Zecchina, *J. Chem. Soc., Faraday Trans.*, 1997, 189.
- 2 H. Pfeifer, D. Freude and M. Hunger, *Zeolites*, 1985, **5**, 274.
 - 3 B. Kraushaar, J. W. de Haan, L. J. M. van de Ven and J. H. C. van Hooff, *Chem. Lett.*, 1986, 1523.
 - 4 G. L. Woolery, L. B. Alemany, R. M. Dessau and A. W. Chester, *Zeolites*, 1986, **6**, 14.
 - 5 M. Hunger, D. Freude, T. Fröhlich, H. Pfeifer and W. Schwieger, *Zeolites*, 1987, **7**, 108.
 - 6 W. Grünert, M. Muhler, K.-P. Schröder, J. Sauer and R. Schlögl, *J. Phys. Chem.*, 1994, **98**, 10920.
 - 7 W. Grünert, M. Muhler and H. Karge, *J. Chem. Soc., Faraday Trans.*, 1996, 701.
 - 8 W. M. Meier and D. H. Olson, *Atlas of Zeolite Structure Types*, Butterworth-Heinemann, London, 1992.
 - 9 G. T. Kokotailo, S. L. Lawton, D. H. Olson and W. M. Meier, *Nature (London)*, 1978, **272**, 437.
 - 10 D. H. Olson, G. T. Kokotailo, S. L. Lawton and W. M. Meier, *J. Phys. Chem.*, 1981, **85**, 2238.
 - 11 A. Zecchina and C. Otero Areán, *Chem. Soc. Rev.*, 1996, **25**, 187.
 - 12 W. Rüdorff and U. Hofmann, *Z. Phys. Chem. B*, 1935, **28**, 351; L. O. Brockway, R. V. G. Ewens and M. W. Lister, *Trans. Faraday Soc.*, 1938, **34**, 1350; S. P. Arnesen and H. M. Seip, *Acta Chem. Scand.*, 1966, **20**, 2711; B. Rees and A. Mitschler, *J. Am. Chem. Soc.*, 1976, **98**, 7918.
 - 13 D. C. Bailey and S. H. Langer, *Chem. Rev.*, 1981, **81**, 109; J. M. Basset and A. Choplin, *J. Mol. Catal.*, 1983, **21**, 95; G. M. Zanderighi, C. Dossi, R. Ugo, R. Psaro, A. Theolier, A. Choplin, L. D'Ornelas and J. M. Basset, *J. Organomet. Chem.*, 1985, **296**, 127; Y. Iwasawa, *Adv. Catal.*, 1987, **35**, 187; J. M. Basset, B. C. Gates, J. P. Candy, A. Choplin, M. Leconte, F. Quignard and C. Santini, *Surface Organometallic Chemistry: Molecular Approaches to Surface Catalysis*, Kluwer, Dordrecht, 1988; H. H. Lamb, B. C. Gates and H. Knözinger, *Angew. Chem., Int. Ed. Engl.*, 1988, **27**, 1127; G. A. Ozin and G. Gil, *Chem. Rev.*, 1989, **89**, 1749; J. M. Basset, J. P. Candy, P. Dufour, C. Santini and A. Choplin, *Catal. Today*, 1989, **6**, 1; J. M. Basset, J. P. Candy, A. Choplin, B. Didillon, F. Quignard and A. Theolier, *The Chemistry for the 21st Century*, eds J. M. Thomas and K. Zamaraev, Blackwell, Oxford, 1991; J. M. Basset, J. P. Candy, A. Choplin, C. Nédéz and F. Quignard, *Mater. Chem. Phys.*, 1991, **29**, 5; T. J. Marks, *Acc. Chem. Res.*, 1992, **25**, 57; S. L. Scott and J. M. Basset, *J. Mol. Catal.*, 1994, **86**, 5; P. Dufour, S. L. Scott, C. Santini, F. Lefebvre and J. M. Basset, *Inorg. Chem.*, 1994, **33**, 2509; C. Otero Areán and C. Mas Carbonell, *Vib. Spectrosc.*, 1995, **8**, 411.
 - 14 R. Szostak, *Molecular Sieves: Principles of Synthesis and Identification*, Van Nostrand Reinhold, New York, 1989.
 - 15 L. Marchese, S. Bordiga, S. Coluccia, G. Martra and A. Zecchina, *J. Chem. Soc., Faraday Trans.*, 1993, 3483.
 - 16 See, for example (a) G. Qin, L. Zheng, Y. Xie and C. Wu, *J. Catal.*, 1985, **95**, 609; (b) L. M. Kustov, V. B. Kazansky, S. Beran, L. Kubelková and P. Jiru, *J. Phys. Chem.*, 1987, **91**, 5247; (c) J. Datka, M. Bozcar and P. Rymarowicz, *J. Catal.*, 1988, **114**, 368; (d) J. Dwyer, *Stud. Surface Sci. Catal.*, 1988, **37**, 333; (e) A. Zecchina, S. Bordiga, G. Spoto, D. Scarano, G. Petrini, G. Leofanti, M. Padovan and C. Otero Areán, *J. Chem. Soc., Faraday Trans.*, 1992, 2959; (f) F. Wakabayashi, J. N. Kondo, K. Domen and C. Hirose, *J. Phys. Chem.*, 1996, **100**, 4154; (g) C. Otero Areán, G. Turnes Palomino, F. Geobaldo and A. Zecchina, *J. Phys. Chem.*, 1996, **100**, 6678.
 - 17 M. B. Sayed, R. A. Kydd and R. P. Cooney, *J. Catal.*, 1984, **88**, 137.
 - 18 M. A. Makarova, K. M. Al-Gefaili and J. Dwyer, *J. Chem. Soc., Faraday Trans.*, 1994, 383.
 - 19 S. Bordiga, C. Lamberti, F. Geobaldo, A. Zecchina, G. Turnes Palomino and C. Otero Areán, *Langmuir*, 1995, **11**, 527.
 - 20 V. B. Kazansky, *Kinet. Katal.*, 1987, **28**, 557.
 - 21 A. Zecchina, E. Escalona Platero and C. Otero Areán, *J. Catal.*, 1987, **107**, 244.
 - 22 C. Morterra and G. Magnacca, *Catal. Today*, 1996, **27**, 497.
 - 23 S. Bordiga, D. Scarano, G. Spoto, A. Zecchina, C. Lamberti and C. Otero Areán, *Vib. Spectrosc.*, 1993, **5**, 69.
 - 24 A. Zecchina and C. Otero Areán, *Catal. Rev.-Sci. Eng.*, 1993, **35**, 261.
 - 25 D. F. Shriver, *J. Organomet. Chem.*, 1975, **94**, 259.
 - 26 C. P. Horwitz and D. F. Shriver, *Adv. Organomet. Chem.*, 1984, **23**, 219.
 - 27 G. C. Pimentel and A. L. McClellan, *The Hydrogen Bond*, W. H. Freeman, San Francisco, 1960.
 - 28 A. Zecchina, E. Escalona Platero and C. Otero Areán, *Inorg. Chem.*, 1988, **27**, 102.
 - 29 P. Ratnasamy, F. P. Babu, A. J. Chandwadkar and S. B. Kulkarni, *Zeolites*, 1986, **6**, 98; G. Paparatto, E. Moretti, G. Leofanti and F. Gatti, *J. Catal.*, 1987, **105**, 227; J. Cejka, B. Wichterlova, J. Krtil, M. Krivanek and R. Fricke, *Stud. Surf. Sci. Catal.*, 1991, **69**, 347.
 - 30 B. A. Morrow and I. A. Cody, *J. Phys. Chem.*, 1976, **80**, 1995.
 - 31 F. Boccuzzi, S. Coluccia, G. Ghiotti, C. Morterra and A. Zecchina, *J. Phys. Chem.*, 1978, **82**, 1298.
 - 32 G. Ghiotti, E. Garrone, C. Morterra and F. Boccuzzi, *J. Phys. Chem.*, 1979, **83**, 2863.
 - 33 G. Boxhoorn, A. G. T. G. Kortbeek, G. R. Hays and N. C. M. Alma, *Zeolites*, 1984, **4**, 15.
 - 34 G. Boxhoorn, R. A. van Santen, W. A. van Erp, G. R. Hays, R. Huis and D. Clague, *J. Chem. Soc., Chem. Commun.*, 1982, 264.
 - 35 G. Engelhardt, B. Fahlke, M. Mägi and E. Lippmaa, *Z. Phys. Chem., Leipzig*, 1985, **266**, 39.

Received 8th July 1996; Paper 6/04775K